Journal of Chromatography A 1710 (2023) 464428

Contents lists available at ScienceDirect

Journal of Chromatography A

journal homepage: www.elsevier.com/locate/chroma

Model based process optimization of an industrial chromatographic process for separation of lactoferrin from bovine milk

Lukas Gerstweiler [a,*], Paulina Schad [b], Tatjana Trunzer [c], Lena Enghauser [c], Max Mayr [d], Jagan Billakanti [e]

[a] The University of Adelaide, School of Chemical Engineering, 5000 Adelaide, Australia
[b] Heidelberg University, 69120 Heidelberg, Germany
[c] Global Life Sciences Solutions Germany GmbH, R&D, 76133 Karlsruhe, Germany
[d] Global Life Sciences Solutions Germany GmbH, Freiburg, Germany
[e] Global Life Sciences Solutions Australia Pty Ltd, Level 11, 32 Phillip St, Parramatta, NSW 2150

ARTICLE INFO

Keywords:
Lactoferrin
mechanistic modeling
process optimization
chromatography
dairy

ABSTRACT

Model based process development using predictive mechanistic models is a powerful tool for in-silico downstream process development. It allows to obtain a thorough understanding of the process reducing experimental effort. While in pharma industry, mechanistic modeling becomes more common in the last years, it is rarely applied in food industry. This case study investigates risk ranking and possible optimization of the industrial process of purifying lactoferrin from bovine milk using SP Sepharose Big Beads with a resin particle diameter of 200 μm, based on a minimal number of lab-scale experiments combining traditional scale-down experiments with mechanistic modeling. Depending on the location and season, process water pH and the composition of raw milk can vary, posing a challenge for highly efficient process development.

A predictive model based on the general rate model with steric mass action binding, extended for pH dependence, was calibrated to describe the elution behavior of lactoferrin and main impurities. The gained model was evaluated against changes in flow rate, step elution conditions, and higher loading and showed excellent agreement with the observed experimental data. The model was then used to investigate the critical process parameters, such as water pH, conductivity of elution steps, and flow rate, on process performance and purity. It was found that the elution behavior of lactoferrin is relatively consistent over the pH range of 5.5 to 7.6, while the elution behavior of the main impurities varies greatly with elution pH. As a result, a significant loss in lactoferrin is unavoidable to achieve desired purities at pH levels below pH 6.0. Optimal process parameters were identified to reduce water and salt consumption and increase purity, depending on water pH and raw milk composition. The optimal conductivity for impurity removal in a low conductivity elution step was found to be 43 mS/cm, while a conductivity of 95 mS/cm leads to the lowest overall salt usage during lactoferrin elution. Further increasing the conductivity during lactoferrin elution can only slightly lower the elution volume thus can also lead to higher total salt usage. Low flow rates during elution of 0.2 column volume per minute are beneficial compared to higher flow rates of 1 column volume per minute.

The, on lab-scale, calibrated model allows predicting elution volume and impurity removal for large-scale experiments in a commercial plant processing over 10^6 liters of milk per day. The successful model extrapolation was possible without recalibration or detailed knowledge of the manufacturing plant. This study therefore provides a possible pathway for rapid process development of chromatographic purification in the food industries combining traditional scale-down experiments with mechanistic modeling.

1. Introduction

Lactoferrin is an iron-binding glycoprotein with a length of 703 amino acids and a molecular size of approximately 80 kDa [1]. It is generally found in various secretory fluids, including serum, tears, semen, and milk, of different mammalian species such as bovine, ovine,

* Corresponding author at: The University of Adelaide, Engineering North Building, North Terrace, 5004 Adelaide, South Australia, Australia.
E-mail address: Lukas.gerstweiler@adelaide.edu.au (L. Gerstweiler).

https://doi.org/10.1016/j.chroma.2023.464428
Received 9 July 2023; Received in revised form 27 September 2023; Accepted 30 September 2023
Available online 2 October 2023

and humans [2]. The concentration of lactoferrin varies greatly among species [3]. Human colostrum contains the highest concentration of lactoferrin (7 g/L), followed by human milk (1 g/L), bovine colostrum, and bovine milk (0.1 – 0.2 g/L) [4,5]. Currently, considering the size of the industry and the global milk volumes produced, bovine milk is the richest source for commercial lactoferrin manufacturing. The global bovine lactoferrin market was valued at United States Dollar (USD) 574.6 million in 2021 and is projected to reach USD 1,850.3 million by 2029, with a compound annual growth rate of 15.7% during the forecast period [6]. Due to increasing awareness of the biological functions of lactoferrin and its potential health benefits, the demand for bovine lactoferrin has steadily increased since 2017. As a result, many global dairy companies are focusing on expanding their lactoferrin production capacities, and since 2012 the world production has doubled from 200-250 tons per annum to expected 550-600 tons per annum in 2023. This expansion may be achieved by increasing the current manufacturing footprint, upgrading technology, building additional plants, or constructing brand-new manufacturing facilities. For example, Synlait Milk (New Zealand) doubled its lactoferrin capacity in 2019 by upgrading its production line. Bega Group Dairy company (Australia) built a brand-new facility in Koroit in 2021, in addition to the existing factory. Beston Global Food Company (Australia) also constructed a brand-new facility in 2021 to replace the existing lactoferrin facility, thereby increasing the manufacturing capacity to 25 metric tons/year from 3 metric tons/year. Westland Milk (New Zealand) has secured New Zealand Dollar (NZD) $70 million for lactoferrin plant expansion in 2023, and Friesland Campina (Netherlands) opened a new lactoferrin facility in 2023, alongside the existing plant, with the capacity to produce up to 80 metric tons/year. Additionally, several new dairy companies with access to milk for lactoferrin manufacturing have built facilities for bovine lactoferrin production. For instance, Nuomi Limited (Australia) established a new lactoferrin facility in 2020, Rokiskio (Lithuania) and Cremo SA (Switzerland) built a new lactoferrin plant in 2021.

Since the demand for bovine lactoferrin has increased, an increasing number of new players are entering the manufacturing pipeline. Customers now have more freedom to choose the origin, source, type, and long-term supply of lactoferrin at a competitive price. However, there are concerns regarding quality and biological activity of bovine lactoferrin due to the lack of global standardization [7]. Currently, the Guobiao (GB) method (GB 1903.17-20160) imposed by the Chinese government for importing lactoferrin to China is the first and ongoing method for assessing lactoferrin quality using a defined high performance liquid chromatography (HPLC) method, which measures lactoferrin purity against the total proteins present in the powder. The minimum requirement for lactoferrin purity according to this standard is 95%, which is now considered the industry standard. In addition to this, several other countries have developed different HPLC methods for a more quantitative estimation of lactoferrin in their powders [8]. However, these protocols have not yet been harmonized across the industry and vary depending on the supplier and customer. Some suppliers can meet the specifications of the GB method but fail to meet other HPLC-based methods, possibly due to different manufacturing practices among suppliers. Besides a high purity, achieving high lactoferrin productivity and recovery is equally important to make the process economically viable. While the high-level lactoferrin purification process is well understood [9], there are several parameters that play a key role in achieving lactoferrin purification with desired purity, high yield, and minimal losses, such as lactoferrin concentration in the feed, residence time, resin dynamic binding capacity, and elution conditions (conductivity, pH, contact time, elution volumes). Ideally, each supplier should invest a significant amount of effort to optimize the purification process parameters for their specific needs. However, uncertainties still exist, such as seasonal variations in feed material or slight changes in elution conditions due to unexpected hardware performance or salt variability or sensor inaccuracy. In such scenarios, manufacturers are uncertain about the quality of lactoferrin they can produce. Sometimes, the product may not meet the required market specifications, leading to suppliers having to sell it at a lower price, or they may reject the batch, generating waste and resulting in a significant financial burden for the manufacturer.

Although costly, chromatography is the most widely used method to purify lactoferrin from bovine milk at large scale [9]. However, optimizing a chromatography process is cumbersome and requires a significant amount of resources, time, cost, and skilled staff. Therefore, not every lactoferrin manufacturer systematically optimizes their lactoferrin process. Mechanistic models to describe the elution behavior in liquid chromatography, based on a set of differential equations to model the underlying transport processes, have gained tremendous interest in the biopharmaceutical industry and academia in recent years, but are not widely applied in the food sciences. The underlying transport models and binding isotherms for a variety of resins, such as ion-exchange, hydrophobic interaction, mixed-mode and affinity matrixes have been developed and applied in a multitude of studies and reviewed in literature [10–13]. Mechanistic modeling enables a deep process understanding which can be used for defining the design space as a key element of quality-by-design approaches and feed forward process control [14,15]. Mechanistic model-based process optimization allows process development with only a minimal number of experiments and is hence an attractive option for cost-efficient and fast process development. This technique became more accessible in recent years by commercial or open source software packages such as GoSilico™ Chromatography Modeling Software and CADET [16].

In our presented case study, GoSilico™ was used to investigate industrial bovine lactoferrin separation in detail with the help of mechanistic chromatography modeling and a limited number of lab scale experiments. Our focus was set on the influence of feed composition, process water pH and flow rate on the adsorption behavior of lactoferrin and impurities on SP Sepharose Big Beads. The calibrated model was screened on model quality and used to define an optimal, seasonal dependent industrial processing range for purifying lactoferrin from bovine milk on SP Sepharose Big Beads. Furthermore, the study investigates the negative impact of unfavourable low process water pH in detail and highlights the reduction of the elution flow rate as a possible process optimisation strategy.

2. Material methods

2.1. Instrumentation and resin

Experiments for model development and validation were conducted on an Äkta™ avant 150 (Cytiva®, Sweden), with a HiScale™ 16/40 column (Cytiva®, Sweden). The column was packed with SP Sepharose Big Beads Food Grade strong cation exchanger (11000829, Cytiva®, Sweden), currently the global standard and used for approximately 70% of the worlds output. The column was packed on manufacturer's recommendation to a final bed height of 13.5 cm (inner diameter 16 mm), which is typically used in commercial plants. A flow rate of 1 column volume per minute (CV/min) was selected as standard flow rate, corresponds to a linear velocity of 810 cm/h. The column was attached to the system with 155 cm length of tubing before and 64 cm length of tubing after the column (internal diameter 0.75 mm, 18111253, Cytiva®, Sweden) plus 6 cm of tubing to the UV sensor (internal diameter 0.5 mm, 18111368, Cytiva®, Sweden). Lactoferrin analytics by analytical cation exchange chromatography was conducted on an Äkta™ go (Cytiva®, Sweden), with a Tricorn 5/50 column filled with 1 mL of SOURCE 15S resin. HPLC experiments were carried out on a Shimadzu UFLC-XR system (pump: LC-20AD-XR, autosampler: SIL-20AXR, diode array detector: SPD-M20A, column oven: CTO-20), with a Vydac Protein C4 column 2.1 × 100 mm, 5 μm (214TP521).

2.2. Chemicals

Non-pasteurized skim milk was obtained from a local dairy company in South Australia, Australia between October 2022 and January 2023, which was aliquoted and stored frozen. Milk was heated to a temperature of at least 48°C in a 50°C water bath before processing. Sodium chloride (NaCl) (SA046), tris-buffer salt (TA034), hydrogen chloride (HCl) (HT020), sodium chloride (NaCl) (SA178), acetonitrile (AA103) and trifluoracetic acid (TFA) (TS181) were obtained from ChemSupply, Australia. MilliQ water was used to prepare buffers. pH adjusted water to mimic variations of water quality in a commercial process was prepared by mixing 80% MilliQ water with 20% Adelaide tap water (hardness: 105 mg/L) and adjusted with HCl and NaOH to either pH 5.5 or pH 7.6.

2.3. Analytics

Lactoferrin concentration was measured by analytical cation exchange chromatography on a 1 mL SOURCE 15S column against analytical lactoferrin standard by peak area integration at 280 nm. Buffer A: 50 mM Tris, pH 7.5, Buffer B: 1 M NaCl, 50 mM Tris, pH 7.5. The exact procedure can be found in the supplementary data.

Reversed phase high pressure liquid chromatography (RP-HPLC) analysis was conducted by gradient elution from 5-75% buffer B over 35 min, at a flow rate of 1 mL/min and column temperature of 40°C. Buffer A: MilliQ water, 0.1% TFA. Buffer B: Acetonitrile, 0.1% TFA. Results were analysed at an absorbance of 280 nm.

Sodium dodecylsulfate polyacrylamide gel electrophoresis (SDS-PAGE) analysis was run under reducing conditions on pre-cast Bolt™ 12% Bis-Tri Plus 1.00 mm X 12 well gels as per manufacturer recommendations (Invitrogen™, USA).

2.4. Chromatography model

This study applies the General Rate Model (GRM) as described in literature, including film diffusion, pore diffusion and surface diffusion in combination with the Steric Mass Action (SMA) model to describe the protein binding, as the underlying model to simulate the elution behaviour [17–19]. While this model is computational expensive it is one of the most detailed models to describe ion exchange chromatography and given the large bead particle size of the chromatographic resin used, transport processes inside the beads will likely have a large influence on elution behaviour.

The interstitial volume in the column is described by a transport dispersive model [18]:

$$\frac{\partial c_i}{\partial t} = -\frac{u(t)}{\varepsilon_{col}}\frac{\partial c_i}{\partial x} + D_{ax}\frac{\partial^2 c_i}{\partial x^2} - \frac{1-\varepsilon_{col}}{\varepsilon_{col}}\left(\frac{3}{r_p}k_{film,i}\left(c_i - c_{p,i}(\cdot,\cdot,r_p)\right)\right) \tag{1}$$

With c_i describing the concentration of a molecule i in the interstitial volume, $c_{p,i}$ the concentration in the liquid pore phase. ε_{col} represent the interstitial porosity and D_{ax} the axial dispersion. $k_{film,i}$ is the film diffusion of component i and $r_p$the particle radius.

The concentration in the pore volume was described by the GRM [18] including surface diffusion as

$$\frac{\partial c_{p,i}}{\partial t} = D_{pore,i}\left(\frac{\partial^2 c_{p,i}}{\partial r^2} + \frac{2}{r}\frac{\partial c_{p,i}}{\partial r}\right) + \frac{1-\varepsilon_{bead}}{\varepsilon_{bead}}D_{solid,i}\left(\frac{\partial^2 q_i}{\partial r^2} + \frac{2}{r}\frac{\partial q_i}{\partial r}\right) - \frac{1-\varepsilon_{bead}}{\varepsilon_{bead}}\frac{\partial q_i}{\partial t} \tag{2}$$

with $D_{pore,i}$ as the pore diffusion coefficient, $D_{solid,i}$ the surface diffusion coefficient and q_i the bound protein concentration on the surface. ε_{bead} is the bead porosity. The adsorption for initial model development without pH dependence was described by the SMA isotherm [19]

$$k_{kin,i}\frac{dq_i}{dt} = k_{eq,i}\left(\Lambda - \sum_j (\nu_j + \sigma_j)q_j\right)^{\nu_i} c_{p,i} - q_i c_s^{\nu_i} \tag{3}$$

Here, $k_{kin,i} = \frac{1}{k_{des}}$ is the kinetic variable [20], $k_{eq,i}$ is the equilibration constant, Λ is the ionic capacity, ν_j is the characteristic charge, σ_j is the shielding factor, and c_s is the salt concentration.

The SMA model can be extended for pH dependence according to Hunt et al. [21] by approximating the influence of the pH on the equilibrium constant and the characteristic charge.

$$k_{eq,i}(pH) = k_{eq,i}e^{k_{eq1,i}\cdot pH + k_{eq2,i}\cdot pH^2} \tag{4}$$

$$\nu_i(pH) = \nu_i + pH\cdot\nu_{1,i} \tag{5}$$

$$pH = pH_{actual} - pH_{ref} \tag{6}$$

2.5. Software

The used mechanistic model equations are implemented in the current version of GoSilico™ Chromatography Modeling Software version 1.13.1 (Cytiva®, Sweden) and solved using this software. The mass transfer and thermodynamic model introduced in the previous section, were implemented in the GoSilico™ software [22]. Parameter uncertainties were calculated via the covariance matrix in the GoSilico™ software. The underlying method derives the covariance matrix over the Fisher information matrix using the parameter sensitivities [22–24]. Data analyses were conducted in Excel. GraphPad Prism 9 and Matlab R2021bwere used for data visualization.

2.6. System and column characterization

The column volume was calculated from the column diameter of 1.6 cm and the final bed height of 13.5 cm.

Total column porosity was determined from the retention volume of a 1 M NaCl solution pulse experiment (300 µL injection volume) at a flow rate of 1 CV/min with 0.4 M NaCl as running and equilibration buffer, subtracting dead volume of the system (measured by the same method using conductivity sensor) and the volume of the connecting tubing.

$$\varepsilon_{total} = \frac{V_{R,cond} - V_{dead,cond} - V_{tubing}}{V_{column}} \tag{7}$$

Interstitial porosity was determined in a similar fashion using 10 mg/mL blue dextran as a tracer and the UV signal.

$$\varepsilon_{col} = \frac{V_{R,UV} - V_{dead,UV} - V_{tubing}}{V_{column}} \tag{8}$$

Bead porosity was calculated from ε_{total} and ε_{col} as

$$\varepsilon_{bead} = \frac{\varepsilon_{total} - \varepsilon_{col}}{1-\varepsilon_{col}} \tag{9}$$

Ionic capacity was derived from titration experiments after equilibrating the column with HCl and running 0.1 M NaOH solution measuring the volume till conductivity breakthrough, according to following formula:

$$\Lambda = \frac{V_{NaOH} * c_{NaOH}}{CV * (1-\varepsilon_{total})} \tag{10}$$

All characterization experiments were conducted in triplicates.

The mean particle diameter d_p of 0.2 mm was obtained from the resin data sheet. Axial dispersion was manually chosen to be 0.01 mm^2/s. In preliminary studies we found that using a calculated apparent axial dispersion, derived from the plate height of a non-penetrating tracer, effectively lumping the two distinct effects longitudinal diffusion and eddy dispersion, leads to insufficient model prediction for variable flow

rates. Using small values for D_{ax} approximating the effective longitudinal diffusion coefficient instead, showed to be beneficial for modeling variable flow rates [17,25-27].

The concentration of lactoferrin in the loading milk was measured by analytical cation exchange chromatography as described above and used to fit the extinction coefficient of lactoferrin, which was then used for all other molecules. The molar mass was set to 78 kDa for all molecules as a generic value. The concentration of all other molecules was fitted against the data of the calibration experiments.

2.7. Model calibration experiments

Model parameters were estimated by the inverse method using data obtained from three gradient elution experiments. The column was loaded with 20.6 column volumes (CV) of skim milk at a flow rate of 1 CV/min and eluted with a 20 CV, 40 CV and 60 CV gradient from 0 to 1.5 M NaCl at a flow rate of 1 CV/min. To extend the model for pH dependence, the obtained model was then further fitted against data of a 40 CV and 60 CV gradient of pH adjusted water at pH 5.5 and 7.6 from 0 to 1 M NaCl (note the reduced NaCl also changes the gradient slope) at a flow rate of 1 CV/min. The NRMSE was used as an error norm and a Levenberg-Marquardt algorithm for fitting.

2.8. Model validation experiments

The developed model was validated against a range of experiments. This included gradient elution of 20, 40 and 60 CV from 0 to 1 M NaCl at a flow rate of 0.3 CV/min, as well as a three-step elution, with an elution volume of 10 CV in each step at a flow rate of 1 CV/min and at a flow rate of 0.3 CV/min. Besides, a step elution with double volume milk load (41.2 CV milk instead of 20.6 CV milk) at a flow rate of 1 CV/min was performed as well as a step elution with pH adjusted water to pH 5.5 and pH 7.6 at a flow rate of 1 CV/min.

All experiments are summarized in Table 1.

2.9. In-silico process optimization

Purity of lactoferrin is typically calculated based on the UV absorbance at 280 nm and only the total purity, not the type of impurity is relevant. As the milk composition is subject to fluctuation, also the amount of impurities to be removed can vary. Based on the binding fraction of milk proteins towards SP Sepharose Big Beads, the required impurity removal to achieve a desired purity of over 95% lactoferrin, the industry purity requirement, can be calculated as following

$$\%_{removal} = 100 - \left(\frac{\%_{LF} \cdot \left(1 - \frac{\%_{Purity}}{100}\right)}{\%_{Impurities}} \right) * 100 \quad (11)$$

The developed model was used for *in-silico* process optimization of a two-step elution process which is typically used in commercial lactoferrin manufacturing with the aim to improve purity and reduce water and NaCl consumption. The first elution step removes impurities and hence is critical for the final purity of lactoferrin as well as product loss caused by coelution, while in the second step lactoferrin is eluted and recovered as the product.

2.10. Large-scale experiments

Large-scale experiments were conducted on-site a dairy company on parallel radial-flow columns with a total column resin volume of 780 L. The elution volume of the lactoferrin recovery step was determined as the peak volume with a cut-off at an absorbance at 280 nm of 50 mAU. No further details can be disclosed, but the experimental conditions were within the investigated boundaries.

3. Results and discussion

3.1. Elution profile, model development and model calibration

Commercial lactoferrin purification differs from most industrial chromatographic processes by not utilizing buffered mobile phases but pure water with only sodium chloride as a modulator. Initial model development was therefore conducted with MilliQ-water neglecting pH deviations. The elution profiles of the three gradient elution experiments are presented in Fig. 1 A-C. Three unresolved peaks of roughly equal size can be identified, an early eluting one, lactoferrin as the last eluting fraction (quantified in offline analytics, not shown) and a peak in between, containing lactoperoxidase (LPO). Furthermore, a small valley between the LPO and lactoferrin peak is visible at an elution gradient of 60 CV. Experiments with pH adjusted water (Fig. 1 D-G) revealed a change in the size of the first two peaks. At pH 5.5 (Fig. 1 D-E) the in between peak becomes more dominant and splits into two peaks at an elution gradient of 60 CV. At pH 7.6 (Fig 1 F-G) the first peak becomes the most dominant peak. From these results and reported contaminants in commercial lactoferrin products it can be concluded that at least five major protein species are eluting: impurity 1, impurity 2, LPO, impurity 3 and lactoferrin, which was used for model developing.

The results of the system and column characterization are summarised in Table 2**.** The measured ionic capacity of 0.221 mmol H^+/mL_{resin} is within the specifications of 0.18-0.25 mmol H^+/mL_{resin} from the supplier. Porosity values are not provided by the supplier but both bead porosity and interstitial porosity of 80.7% and 34.8% respectively seem to be in reasonable range and similar to previously reported values [28, 29]. Fitted model paramteres obtained by inverse method for the GRM model with SMA binding, as well as the extension parameter to account for pH dependence are presented in Table 3.

The model without pH extension (Fig 1 A-C) using non pH adjusted water nicely describes the experimental data for all three gradients. Peak positions, shape, valleys and heights are adequatly described, only at the steepest gradient of 20 CV (Fig. 1 A) the model cannot describe the shallow valley between the first two peaks in the experimental data precisely. As the model was calibrated without any offline analytics, it is worth mentioning that fitting the model against the experimental data was challenging in particular for the minor impurity 3, and the highly overlapping impurities 1 and 2. Fitting all parameters simulatenously was not possible. We therefore concentrated first on the peak position influenced by charge, equilibrium and kinetic and then on peak shape. This approach has been conducted in a repetitive manner with increasingly narrower bounds for the model parameters until

Table 1
Calibration and validation experiments.

	Number	Loading amount milk	Elution conditions	Flow rate	pH
Calibration	3	20.6 CV	20, 40, 60 CV gradients	1 CV/min	5.5
	2		40, 60 CV gradients	1 CV/min	
	2		40, 60 CV gradients	1 CV/min	7.6
	3	20.6 CV	20, 40, 60 CV gradients	0.3 CV/min	
Validation	2	20.6 CV	Three-step elution	0.3 and 1 CV/min	
	1	41.2 CV	Three-step elution	1 CV/min	
	2	20.6 CV	Three-step elution	1 CV/min	5.5 and 7.6

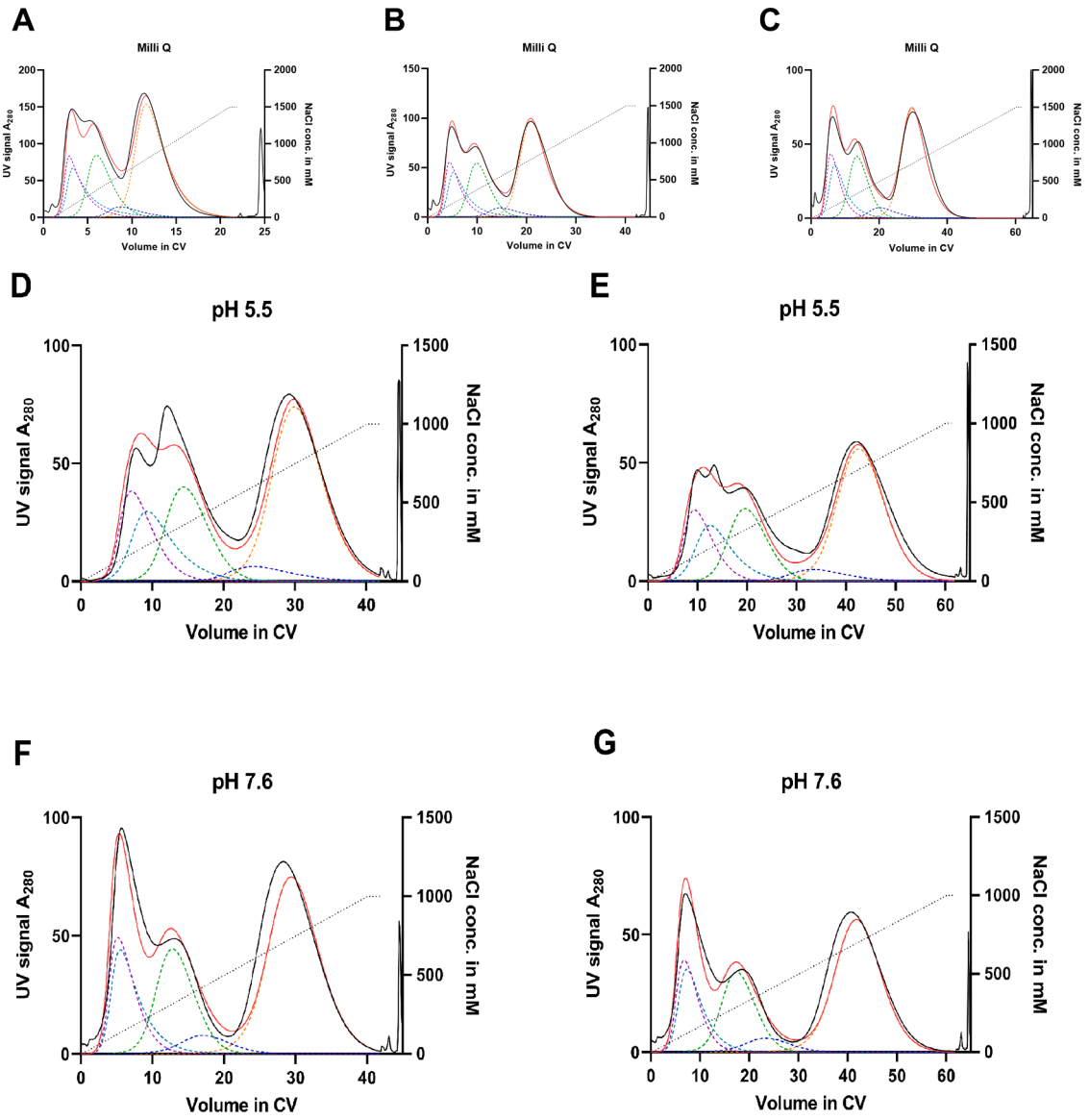

Fig. 1. Experiments for model calibration. A: Milli Q water, 20 CV gradient. B: Milli Q water, 40 CV gradient. C: Milli Q water, 60 CV gradient. D: Water adjusted to pH 5.5, 40 CV gradient. E: Water adjusted to pH 5.5, 60 CV gradient. F: Water adjusted to pH 7.6, 40 CV gradient. G: Water adjusted to pH 7.6, 60 CV gradient. Flow rate in all experiments 1 CV/min. (–) represents the measured UV_{280nm} signal; all other curves show simulated results: (–) UV_{280nm} signal, (—) Lactoferrin, (—) LPO, (—) Impurity 1, (—) Impurity 2, (—) Impurity 3, (●●●) NaCl.

Table 2
Parameters used to characterize the system column. Values highlighted by * are measured.

Parameter	Value	Unit
*Bead porosity ε_{Bead}	80.7	%
*Particle diameter d_p	0.2	mm
*Ionic capacity Δ	0.221	M
*Interstitial porosity ε_i	34.8	%
*Total porosity ε_t	87.42	%
Axial dispersion	0.01	mm^2/s
*Bed height	13.5	cm
*Inner diameter	1.6	cm
pH reference	6.55	[-]

sufficiently visual fitting results were achieved. Extending the model for pH dependence, including all three pH variables of the model (Charge 1, Equilibrium 1 and Equilibrium 2) lead to bad results and illogical model behaviour. The used pH model describes changes in the equilibrium constant with a linear and quadratic term, as well as changes in the charge with a linear term, and can therefore be seen as a polynomal curve fitting which bears the risk of oscillation between the measurement points. In the relatively small pH window from pH 5.5 to pH 7.6, dramatic changes in the protein charge and retention behavior are not expected. We therefore decided to only include linear changes in the equilibrium (Equilibirum 1) and neglect the quadratic term, as well as changes in the charge of the proteins [30,31]. The developed model describes the experimental data well, ecspecially at pH 7.6, while at pH 5.5 minor deviations exist at the early eluting impurities. However, we decided that the first two elution species do not have the highest priority to be modeled precisely as they are not coeluting with the target protein, lactoferrin, and therewith do not affect the elution behavior directly. The calibrated, pH-dependent model is hence acceptable. Furthermore, the valley between lactoferrin and LPO is not perfectly described at pH 5.5 and a 60 CV gradient. At this place it is worth to mention, that the mobile phase (process water) is not buffered in commercial lactoferrin processing. We identified that the eluting proteins highly influence the pH value of the mobile phase (data not shown) which might further

Table 3
Model parameters obtained by inverse method of fitted model with additional pH dependecy. (Concentration of lactoferrin as a reference value was measured as described).

Paramater	Lactoferrin	LPO	Impurity 1	Impurity 2	Impurity 3	Unit
Film diffusion	0.090	0.020	0.006	0.009	0.048	mm/s
Pore diffusion	8.009e-5	1.489e-4	4.276e-5	7.920e-5	1.390e-4	mm^2/s
Surface diffusion	2.297e-5	1.035e-5	1.330e-5	9.387e-6	7.676e-6	mm^2/s
Charge (SMA)	8.527	4.120	3.687	3.140	4.074	[-]
Equilibrium (SMA)	1.187e6	148.241	6.754	4.200	1167.29	[-]
Kinetic (SMA)	1.763	0.070	1.810e-6	4.162e-5	0.616	[-]
Shielding	52.544	51.309	57.930	55.723	29.455	[-]
Concentration	0.137	0.060	0.047	0.045	0.014	g/l
Extinktion	92867.6	92867.6	92867.6	92867.6	92867.6	AU/M/cm
Charge 1 (pH)	0	0	0	0	0	pH^{-1}
Equilibrium 1 (pH)	-0.125	-0.350	-1.265	-0.710	-1.026	pH^{-1}
Equilibrium 2 (pH)	0	0	0	0	0	pH^{-2}

challenges the modeling of lactoferin separation processes as this changes the charge of the protein species and is not accounted for in the used model equations.

The developed model uses all possible diffusion paramters of the GRM, including surface diffusion, pore diffusion and film diffusion as the used resin SP Sepharose Big Beads has a mean particle diameter of 0.2 mm and hence particle mass transfer should be of great importance. This, however, might bear the risk of over-parameterization and parameter correlations. A detailed discussion about model quality follows in the model validation section.

3.2. Model validation

The model was evaluated against a range of experiments not used for model calibration (see Table 1). This included gradient elution at three gradients with different slopes and a much lower flowrate of 0.3 CV/min, which is typically used in industrial lactoferrin processes. However, to speed up the model calibration we decided to perform the calibration experiments at 1 CV/min and study, if it is possible to extrapolate the calibrated model to industrial applied flow rates. Beside the linear gradient experiments, industrial favoured step elution experiments at 0.3 CV/min and 1 CV/min, as well as step elution experiments at pH 5.5 and 7.6 were performed. The three-step experiment was selected to investigate an optimized process that allows fractioning pure LPO and lactoferrin, which we expect can be an increasing demand in future industrial processes. A step elution experiment with double load was evaluated to verify higher resin loadings. The chromatograms of these experiments as well as the model predictions are presented in Fig. 2. The experiments of elution with water at 1 CV/min, pH 5.5, and pH 7.6 were also analysed by SDS-PAGE (Fig. 3) and RP-HPLC (data partially provided in supplementary data).

The experiments with a reduced flow rate (Fig. 2 A-D) unveil that the developed model can accurately predict elution behaviour at these highly reduced elution flow rates. The elution behaviour of the three species of main interest lactoferrin, LPO as well as impurity 3 are well predicted in gradient elution experiments, albeit the lactoferrin peak retention volume is between 3.56 % and 4.98 % different to the measured value. To a much smaller extend this deviation and trend between measured and predicted values and can also be observed for LPO. At the 20 CV gradient experiment (Fig. 2 A) the measured LPO peak is slightly earlier than the simulated one, while in the 60 CV gradient experiment (Fig. 2 C) the measured signal is slightly later. This can be caused by pumping regulations and fluid dynamic effects or the model parameters. As this effect is small and not visible in the step experiment, it is a neglectable deviation. The three-step elution experiments match nicely for the steps at medium and high conductivity, at which the target components LPO and lactoferrin elute. Although the peak position of the early eluting species impurities 1 and 2 are adequately predicted, the peak shape differs as the model predicts a much higher and narrower peak than what was measured. A similar trend can be observed for the other step elution experiments at a flow rate of 1 CV/min, double load or with pH adjusted water of pH 5.5 and pH 7.6 (Fig. 2 E-H). A plausible explanation for this shortcoming is, that the early eluting fractions are in fact a mixture of many more species, which can be seen in SDS-PAGE analysis (Fig. 3 lane 1), and a lumping into two species is insufficient. However, as we defined that the proper elution peak shape of impurity 1 and 2 is neglectable (see discussion in model calibration) all evaluation experiments fulfill the demands. The peaks containing LPO and lactoferrin are well predicted by the model. Investigating impurity 3 a bit closer, showed that with water adjusted to pH 5.5 (Fig. 2 G) the model predicted that the majority of impurity 3 is coeluting with lactoferrin, and this impurity can also be observed by SDS-PAGE analysis as a band at 14 kDa size in lane 6 in Fig. 3. At pH 7.6 (Fig. 2 H) the model predicted no impurity 3 in the lactoferrin peak, and this is also verified on lane 9 Fig. 3, in which no impurity could be detected by SDS-PAGE. For non-adjusted water (Fig. 2 E) the model predicts co-elution of impurity 3 with lactoferrin, which can also be detected by SDS-PAGE on lane 3 Fig. 3.

The results of SDS-PAGE analysis were also verified by RP-HPLC (data provided in supplementary data). Detecting no impurities in lactoferrin obtained with a water pH of 7.6 and a single impurity contamination at pH 5.5, as predicted by the model.

In summary, it can be concluded that the elution behavior of the main species of interest (lactoferrin, LPO and impurity 3) can be well predicted outside the calibration range. As the early eluting species are in fact a mixture of multiple proteins, the approach of lumping them into two seems to be sufficient for our approach. However, its deviations in elution time shows the limitation of modeling complex and unresolved peaks.

Following good modeling practices the parameter uncertainty was evaluated [32,33]. The confidence intervals for lactoferrin and LPO at the confidence level of 95% are presented in Table 4. The validation experiments showed that the early eluting species impurity 1 and impurity 2 are not adequately described by the developed model and hence excluded from statistical analysis. As previously described the parameter uncertainty increases for species that only account for a minority of the model output, which we also observed in our experiments for the minor impurity 3 (data not presented in Table 4) [32]. This opens up the questions if this approach alone is suitable to validate the model quality for minor impurities. It has been shown, that spiking with impurities to increase its concentration, can lead to a higher accuracy of the model [34]. This approach, however, is only applicable if purified impurities are available and hence impracticable in our experiments. The confidence intervals of lactoferrin and LPO show, that the errors for pore diffusion, surface diffusion, charge and equilibrium are very low (<10%), fulfilling the demand of a well-calibrated model with high model quality. However, film diffusion, kinetic and shielding show a higher uncertainty. A high uncertainty in predicting the kinetic parameter and shielding has been previously described [32,35]. It has also been reported that the kinetic parameter has only a minimal

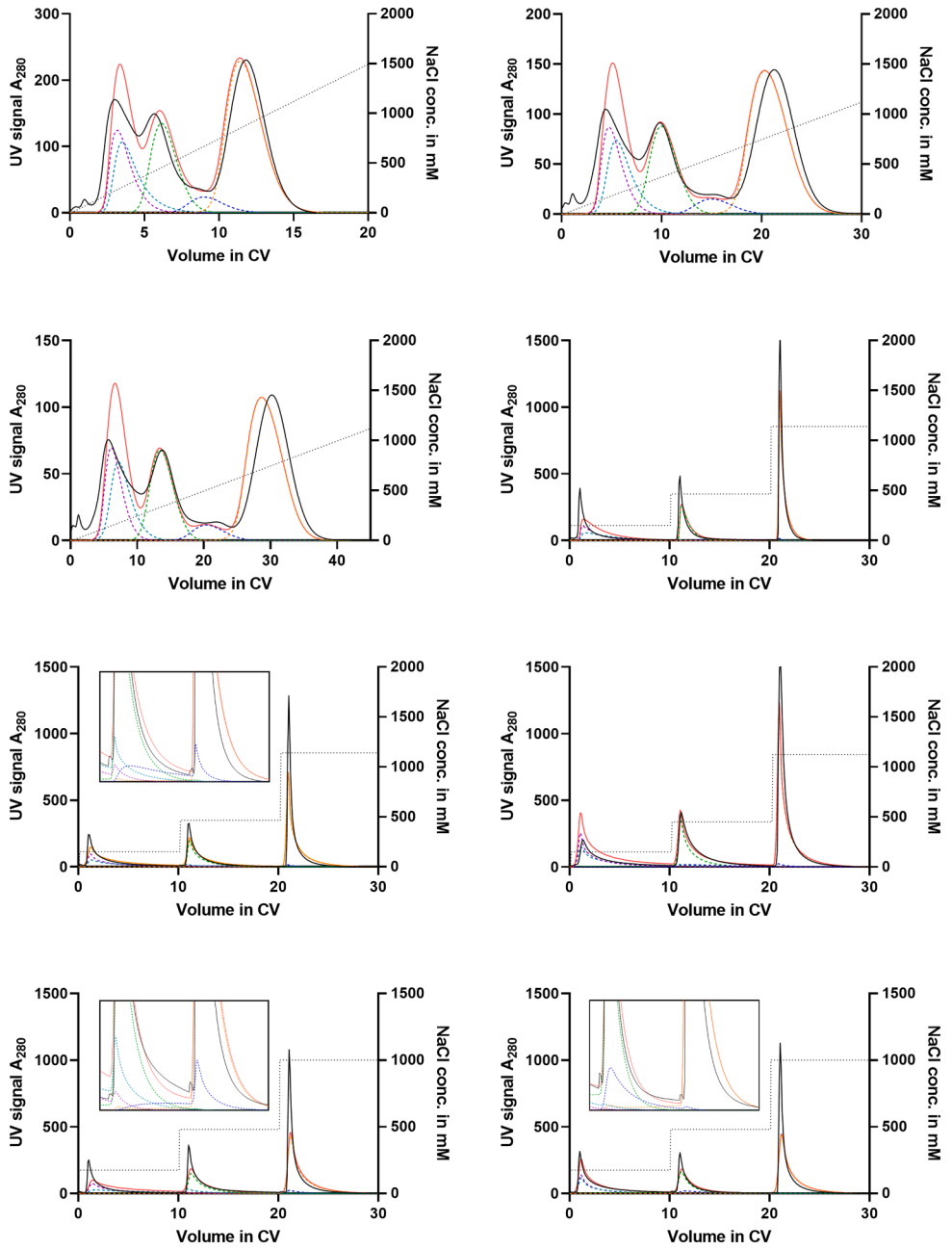

Fig. 2. Model validation experiments and model predictions. A: 20 CV gradient elution 0-1 M NaCl, flow rate 0.3 CV/min. B: 40 CV gradient elution 0-1M NaCl, flow rate 0.3 CV/min. C: 60 CV gradient elution 0-1M NaCl, flow rate 0.3 CV/min. D: Step elution, flow rate 0.3 CV/min. E: Step elution, flow rate 1 CV/min. F: Step elution double load, flow rate 1 CV/min. G: Step elution, water adjusted to pH 5.5, flow rate 1 CV/min. H: Step elution, water pH adjusted to pH 7.6, flow rate 1 CV/min. Enlargements are of peak 2 and peak 3.
(–) represents the measured UV_{280nm} signal; all other curves show simulated results: (–) UV_{280nm} signal, (—) Lactoferrin, (—) LPO, (—) Impurity 1, (—) Impurity 2, (—) Impurity 3, (●●●) NaCl.

influence of the model result [36]. Similarly, gradient elution experiments alone might be insufficient to predict the shielding factor and require additional breakthrough data, or elution data at high load [35,37]. Furthermore, including step elution experiments during model calibration can help to lower the uncertainty of kinetic parameters. A certain uncertainty in the film diffusion is acceptable as the film diffusion is typically assumed to be high and not rate limiting and hence of minor relevance modeling preparative chromatography [36]. It is interesting that the confidence interval data corresponds well with the experimental validation. The errors for the two main species LPO and lactoferrin are very low, and the experimental validation also show a high agreement with the model prediction.

Based on the Pearson coefficients calculated for lactoferrin we observed a very high correlation between charge and equilibrium and of the film diffusion with the kinetic. The correlation of charge and equilibrium has been described in literature before and might be a shortcoming of the SMA model [32,35]. The correlation between film diffusion and kinetic might be explained by the high uncertainties of these two parameters (Table 4). The surface diffusion is correlated to multiple other parameters and showed a high correlation with film diffusion and a moderate correlation with the pore diffusion and the kinetic. This is a sign that this parameter can not be uniquely estimated and might be of low mechanistic value altough the surface diffusion is within range of other reported values [27,38,39]. It has been shown that

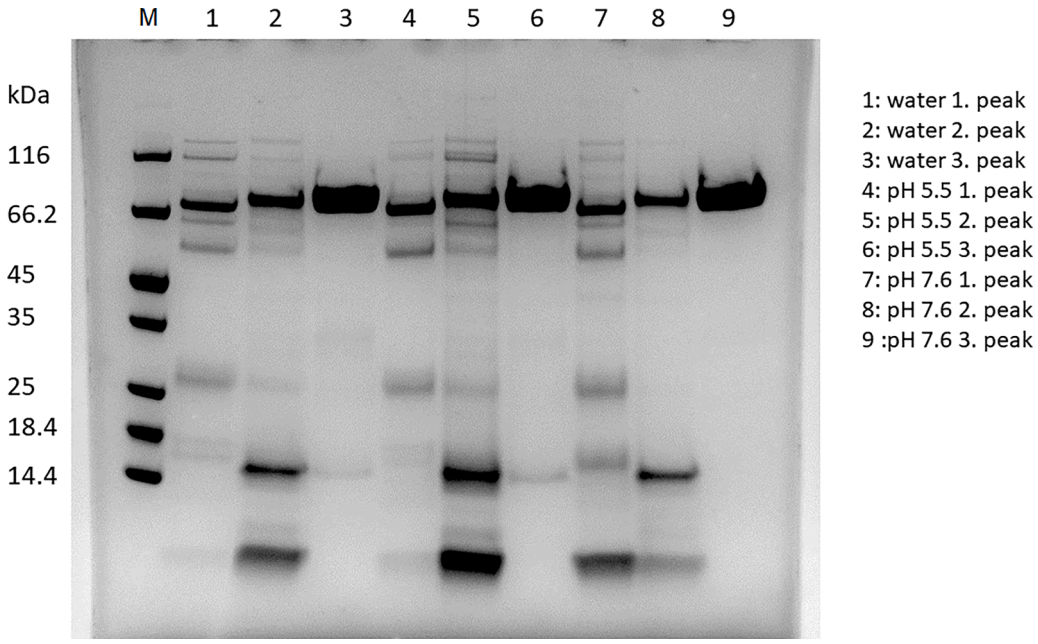

Fig. 3. SDS-PAGE analysis of model validation experiments presented in Fig. 2. M: Marker, Lane 1: Peak 1, Fig. 2 E. Lane 2: Peak 2, Fig. 2 E. Lane 3: Peak 3, Fig. 2 E. Lane 4: Peak 1, Fig. 2 G. Lane 5: Peak 2, Fig. 2 G. Lane 6: Peak 3, Fig. 2 G. Lane 7: Peak 1, Fig. 2 H. Lane 8: Peak 2, Fig. 2 H. Lane 9: Peak 3, Fig. 2 H.

Table 4
Confidence intervals for the calibrated model parameters of the two species of main interest lactoferrin and LPO at a confidence level of 95 % derived from the covariance matrix.

Parameter	Value	Error
Film diffusion – Lactoferrin	0.09043 mm/s	222.31 %(log)
Film diffusion – LPO	0.02000688 mm/s	29.84 %(log)
Pore diffusion – Lactoferrin	8.009 mm^2/s	1.39 %(log)
Pore diffusion – LPO	1.489e-4 mm^2/s	2.91 %(log)
Surface diffusion – Lactoferrin	2.297e-5 mm^2/s	2.58 %(log)
Surface diffusion – LPO	1.035e-5 mm^2/s	7.77 %(log)
Charge – Lactoferrin	8.527 [-]	4.65 %
Charge – LPO	4.120 [-]	9.12 %
Equilibrium – Lactoferrin	1.187e6 [-]	4.55 %(log)
Equilibrium – LPO	148.241 [-]	2.53 %(log)
Kinetic – Lactoferrin	1.763 [-]	129.80 %(log)
Kinetic – LPO	0.070 [-]	62.73 %(log)
Shielding – Lactoferrin	52.544 [-]	70.48 %
Shielding – LPO	51.309 [-]	154.30 %

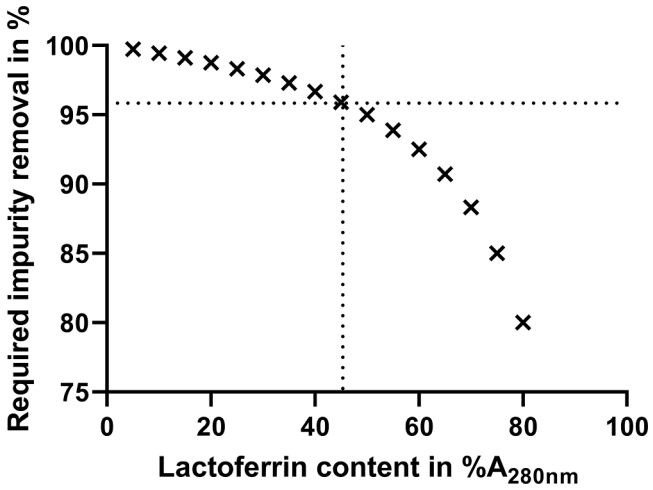

Fig. 4. Required impurity removal considering the binding fraction of bovine milk towards Sepharose SP Big Beads to achieve a final lactoferrin purity of 95% as a function of lactoferrin content in $\%A_{280nm}$ adsorption. No lactoferrin loss and a complete recovery is assumed. The dotted line highlights the milk used in this study as a reference.

the surface diffusion is dependent on the binding affinity/desorption rate and can be described as a function of the ionic strength during elution to obtain accurate predictions in ion exchange chromatography, which is a more realistic implementation of this effect [25,36,38,40].

3.3. Process optimization

Food grade protein prepartions used for oral consumption have less strict purity requirements compared to pharmaecutical grade proteins, and the main quality attribute of the final product is purity, typically determined by HPLC, with commercial products compelled to exceed a protein purity of 95%. Aggreagtes, dimers and variantions in the apo-lactoferrin/holo-lactoferrin ratio are typically not measured by HPLC methods [7]. Lactoferrin concentration and impurity profiles in bovine milk can vary greatly as lactoferrin concentrations between 31.78 mg/L and 485.64 mg/L have been reported [41]. If only the binding protein fraction of bovine milk on Sepharose SP Big Beads is considered and a 100% recovery of lactoferrin is assumed, the required amount of impurity removal to achieve a 95% purity in the endproduct can be easily calculated according to Eq. 11. The results are presented in Fig. 4. It is obvious, that a high lactoferrin concentration will require a much lower impurity removal, compared to a milk with high ratio of impurites to lactoferrin. The milk used in this study showed to have a lactoferrin content of 45.3% of the binding fraction, which would require an impurity removal of about 95.9% to meet the quality requirements. This is however, only true under the assumption that all lactoferrin can be recovered, therefore, during process development a saftey factor should be added.

Due to milk being highly variable, impossible to influence on a process level and different to the elution solution this study did not investigate the loading conditions but focus solely on optimising the elution process. The model was first used to investigate the first elution step (low salt elution) which determines the effectiveness of impurity removal and lactoferrin purity of the final product to find the optimal conductivity. Fig. 5 A illustrates the impurity removal as well as the

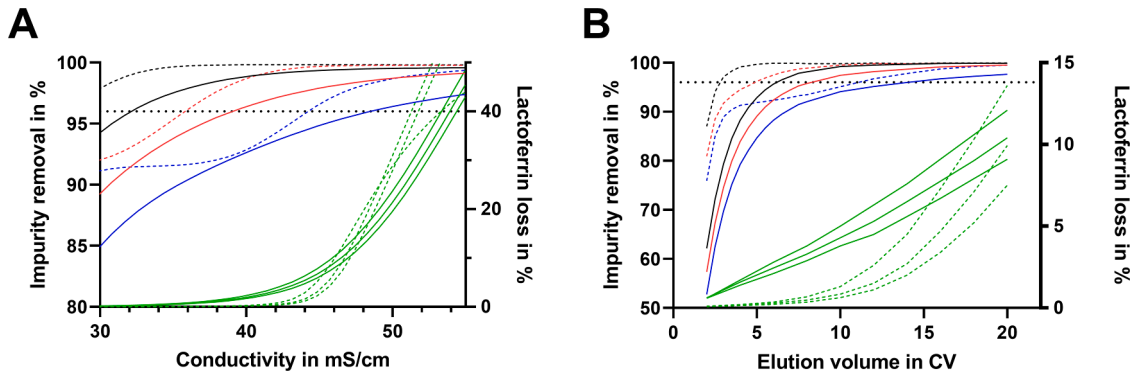

Fig. 5. Model based investigation of 1st elution step. A) Impurity removal and lactoferrin loss as a function of conductivity, for a step length of 10 CV. B) Impurity removal and lactoferrin loss as a function of the elution volume for a conductivity of 43 mS/cm. (-) pH 7.6, flow rate 1 CV/min. (—) pH 7.6, flow rate 0.2 CV/min. (-) pH 6.5, flow rate 1CV/min. (—) pH 6.5, flow rate 0.2 CV/min. (-) pH 5.5, flow rate 1 CV/min. (—) pH 5.5, flow rate 0.2 CV/min. (-) lactoferrin loss at pH 5.5, 6.5, and 7.6, flow rate 1 CV/min. (—) lactoferrin loss at pH 5.5, 6.5, 7.6, flow rate 0.2 CV/min. Dotted line highlights the required impurity removal for the milk used in this study as a reference.

lactoferrin loss as a function of the elution conductivity for a step length of 10 CV at flow rates of 0.2 CV/min and 1CV/min. An increase in the water pH from 5.5 to 7.6 dramatically increased the impurity removal for a given conductivity. For example at a conductivity of 30 mS/cm and a flow rate of 1 CV/min only 85% impurties are being removed at a pH of 5.5, while nearly 95% are being removed at a pH of 7.6. A 96% impurity removal would require a conductivity of 48.5 mS/cm at pH 5.5, a conductivity at which significant loss of lactoferrin occures. A reduction in the flow rate to 0.2 CV/min also increases the impurity removal signifiantly at all pH values. The lactoferrin loss however, is similar at all pH values. Significant losses >1% start to occur at a conductivity of 43 mS/cm at a flow rate of 0.2 CV/min and at 38 mS/cm at a flow rate of 1 CV/min. Unexpectedly, a higher flow rate of 1 CV/min leads to higher losses of lactoferrin at conductivities below 47 mS/cm and lower losses at higher conductivies. Although counterintuitive, this might be explained by diffusion limitations, that can limit re-binding at lower conductivities and a diffusion out of the pores at higher conductivites at the short residence time.

For process optimization it is also relevant to minimize the elution volume. Fig. 5 B shows the impurity removal as a function of the elution step length at a conductivity of 43 mS/cm. Increasing the pH from 5.5 to 7.6 can lower the elution volume required to reach a desired impurity removal dramatically. At a flow rate of 0.2 CV/min the elution volume can be reduced from approximately 11 CV to 3 CV to achieve a 96% impurity removal, and at a flow rate of 1 CV/min from 12 CV to 6 CV. An increased pH does affect the loss in lactoferrin comparatively little for elution volumes below 10 CV but becomes more significant with higher elution volumes. A higher flow rate leads to a higher loss of lactoferrin, although this effect inverts at very high elution volumes. From the simulations it can be concluded that to meet purity requirements, a loss in lactoferrin has to be accepted at higher flow rates of 1 CV/min even at higher water pH values. Reducing the flow rate to 0.2 CV/min leads to a reduction of lactoferrin loss, and a pH above 6.5 allows to obtain the required purity levels without significant losses of lactoferrin. However, at low pH values of 5.5 product losses need to be accepted even at very low elution flow rates.

To further illustrate this effect and simplify decision making, the boundaries for different levels of impurity removal and product loss, as well as neccessary elution volumes and elution times have been illustrated in Fig. 6. For a fixed elution volume of 10 CV it can be seen that at a flow rate of 0.2 CV/min (Fig. 6 A) a process window opens above a pH of 6.5 that allows for 99% removal of the impurites while also minimising lactoferrin losses to below 1%. If an impurity removal of 95% is sufficient a process water of pH 5.5 is also acceptable. At a higher flow rate of 1 CV/min (Fig. 6 B), a 99% removal of the impurities will always lead to high losses of lactoferrin, even at a pH of 7.6, the loss will be around 5%. If a 95% removal is sufficient a pH of at least 6.7 is required to avoid losses in lactoferrin. The benefit of a reduced flow rate is also clearly visible by comparing the required elution volume for a possible operational space defined for 95% impurity removal and a lactoferrin loss < 5% (Fig. 6 C and Fig. 6 D). A low flow rate of 0.2 CV/min opens up a much wider operational space while also reduces the required elution volume by up to nearly 50% for favourable conditions at higher water pH and higher conductivities. For example at a water pH of 7.5 and a conductivity of 44 mS/cm the elution volume decreases from 6.6 CV at a flow rate of 1 CV/min to 3.3 CV at a flow rate of 0.2 CV/min. At low pH conductivities the reduction is however less significant. The reduction in flow rate does however increase the elution times, and hence decrease productivity which is illustrated in Fig. 6 E and Fig. 6 F. While the impact is less severe at a water pH above 6.5, in which the elution times increases from 8 to 20 minutes, caused by a strongly reduced elution volume, the elution time can increase nearly five times at the most unfavourable conditions at a pH of 5.5 and a conductivity of 40 mS/cm.

The presented data highlights the challenges of process development if the water pH is at the lower end of the investigated range from pH 5.5 to 7.6, as the conductivity required to achieve a desired impurity removal inevitably leads to high product losses. Lowering the flow rate is generally beneficial and a possible strategy to improve the purification process as it can also lower the required elution volume. However, a reduced flow rate also leads to extended processing times, in particular at lower pH values, while at higher pH values the reduction in elution volume partially balances out the reduced flow rate.

After impurity removal, the lactoferrin is recovered with a high conductivty elution step. The three main objectives that need to be achieved are a high recovery of lactoferrin, a low elution volume which is beneficial for the subsequent buffer exchange step, and a low salt consumption to minimize raw material costs. Initial simulations unveiled that the influence of the water pH on lactoferrin elution in the recovery step can be neglected and for simplicity reasons only data for a pH of 6.5 is presented. As can be seen in Fig. 7 A, an increase in conductivity to around 100 mS/cm strongly reduces the required elution volume for a 98% recovery. Higher conductivities only decrease the elution volume slightly. As expected, a reduction in the flow rate decreases the required elution volume as well. However, the gain of using very low flow rates is somewhat limited due to increased production times (Fig. 7 C). A reduction of the flow rate from 0.2 CV/min to 0.1 CV/min (at 120 mS/cm) only reduces the elution volume from 2.28 CV to 1.80 CV (21%) while Increasing the elution time from 11.4 minutes to 18.0 minutes (57.9%). Using this data to calculate the required mass of NaCl (presented in Fig. 7 B) for a 98% product recovery, unveils that there is an optimal conductivity at which the salt requirement is the lowest. This was found to be at a conductivity of 95 mS/cm and is

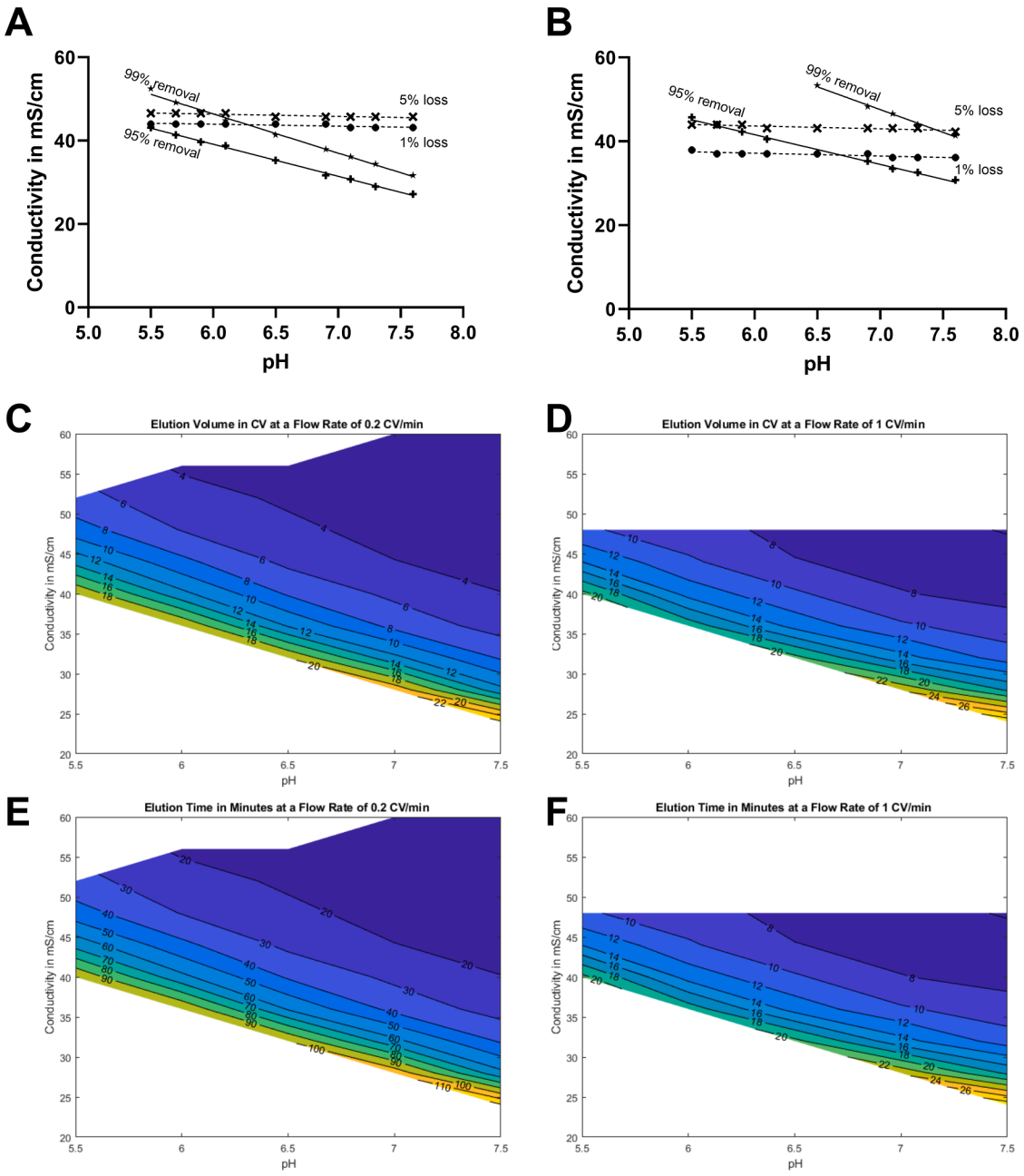

Fig. 6. Impurity removal and lactoferrin loss at a step elution of 10 CV at different pH and conductivity. Dotted lines highlight the conductivty at which 1% (•) or 5% (x) loss of lactoferrin occurs. Solid lines represent the conductivity required to achieve a minimum of 95% (+) and 99% (*) impurity removal. A) Flow rate of 0.2 CV/min. B) Flow rate of 1 CV/min. Required elution volume and possible operational space for 95% impurity removal at a flow rate of 0.2 CV/min (C) and 1 CV/min (D). Required elution time in minutes and possible operational space for a 95% impurtiy removal at a flow rate of 0.2 CV/min (E) and 1CV/min (F). Conditions with elution volumes > 30 CV and lactoferrin losses > 5% are excluded from the data.

independent of the flow rate. Higher conductivities can only slighly reduce the elution volume, but lead to an overall higher salt consumption which means increased raw material costs. The biggest decrease in salt consumption can be achieved by lowering the flow rate. At the optimal conductivity of 95 mS/cm a decrease in the flow rate from 1 CV/min to 0.1 CV/min decreases the salt consumption by nearly 70%, however it also increases the elution time 3.8 times to 26 minutes.

As a conclusion, the developed model can also be used as a powerful guidance to establish the design space of process parameters that provide assurance of quality including the normal operating range (NOR) and the proven acceptable range (PAR) as part of a quality by design workflow. Focusing the industrial challenge of reaching at least 95% lactoferrin purity by keeping the product loss minimal, the acceptable process parameter range would be fulfilled when elution takes place at minimum 43 mS/cm at low flow rate of 0.2 CV/min and an elution volume of 10 CV. To stand seasonal fluctuations of the regional dependent pH, the normal operation range can be adapted with the help of GoSilico^{TM} software.

3.4. Large-scale experiments

While model validation showed that the developed model can accurately predict lab-scale experiments, it is also of high interest to investigate if findings can be transferred to large-scale industrial set-ups. Fig. 8 presents the elution volume of the lactoferrin recovery step at different conductivites measured in a commercial plant, and the

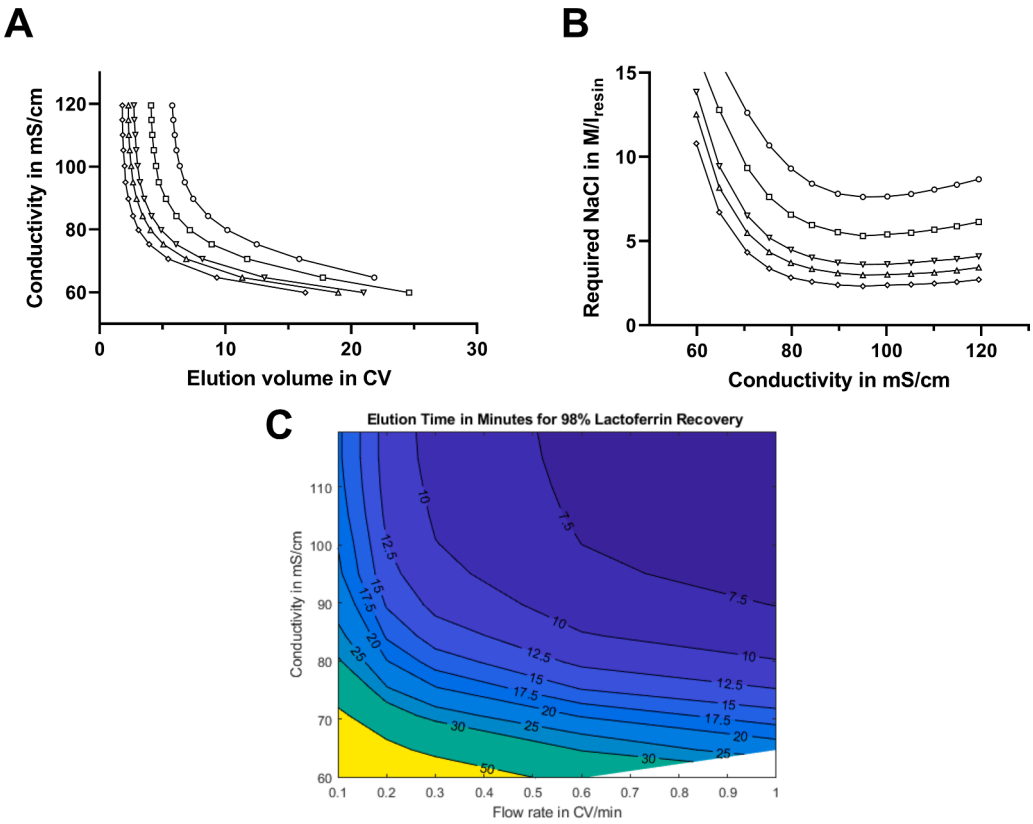

Fig. 7. Investigation of the high conductivity elution step for recovery of lactoferrin. A) Required elution volume at different conductivities to recover 98% of the bound lactoferrin. B) Required mass of NaCl as a function of conductivity to achieve a 98% recovery. (○) flow rate 1 CV/min, (□) 0.6 CV/min, (▽) 0.3 CV/min, (△) 0.2 CV/min, (◇) 0.1 CV/min. C) Elution time in minutes to recover 98% of the bound lactoferrin at different flow rates and conductivities.

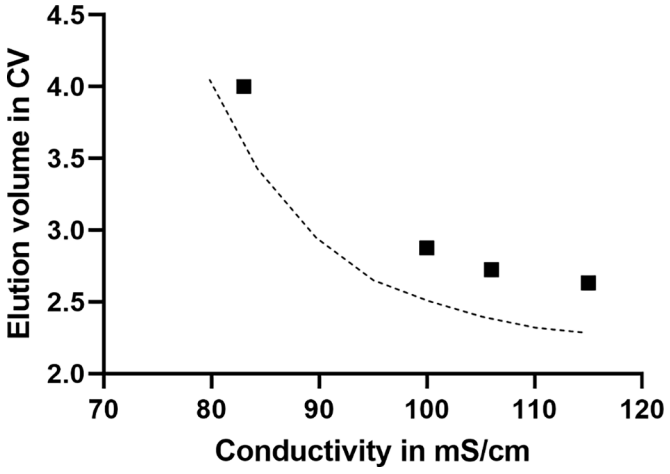

Fig. 8. Required elution volume of the lactoferrin recovery step at different conductivities at a commercial plant. (■) measured values at manufacturing plant. (—) model predictions from lab-scale experiments.

simulated values for a flow rate of 0.2 CV/min. The measured elution volumes are slighlty higher by approximatley 0.5 CV than the predicted values. The overall trend however, is well described by the model. The higher elution volume in large scale experiments can be explained by the much larger dead volumes in the system compared to laboratory equipment. These are caused by extensive piping and large mixers, inducing a stronger backmixing and hence a peak broadening. Furthermore, radial flow columns were used in large-scale experiments compared to axial flow packed bed chromatography columns during lab scale set-up.

It has also been investigated if conditioning of the process water pH is a viable option to increase the product purity and process robustness, as predicted by the model. Product purity was measured by analytical cation exchange chromatography. An increase of the process water pH from pH 5.6 to 6.9, with other process parameters remaining constant, increased the lactoferrin purity from 92.4% to 96.4%, similar to the model predictions.

From the above results it is clear, that the overall trend in large scale experiments can be well predicted with a model developed in lab-scale without knowing the system in detail, following standard scale down principles of same bed height and same linear flow velocity. And hence optimal process parameters such as conductivity and flow rate will likely be similar in a commercial plant. As a result, this approach can be a viable option for low-cost and geographical independet process development. However, every plant will show a different behavior caused by the exact plant dimensions. Depending on the objective and ressources two strategies can be applied to use the findings for a large-scale process. If a complete characterization at the manufacturer site is impracticable, the findings from the lab-scale model can be used as a starting point during commissioning and the optimal plant specific process parameters can be evaluated with a limited number of experiments. However, to predict real time conditions and the real optimum process parameters of the plant, it is required to describe each manufacturer specific system properly and recalibrate the model to account for the differences between the scales and set-ups. This can require additional on-site experiments by skilled workers and be a challenge in the food-industry that must be decided on a case-by-case basis.

4. Conclusion

A predictive mechanistic model based on the general rate mode with SMA binding and pH extension was successfully developed for bovine

lactoferrin purification from skim milk. The predictive model demonstrated a solid approach for optimizing the lactoferrin purification process, predicting an optimal conductivity of 43 mS/cm in the low salt elution step and 95 mS/cm in the high salt elution step for minimal salt consumption. It also demonstrated the benefit of more efficient impurity removal at an elution pH above pH 6.5 and reduced flow rates during elution, minimizing buffer consumption. The findings agreed well with large scale experiments on a commercial plant without knowing the exact plant dimension, albeit large scale experiments showed a larger elution volume. The offset is not surprising considering increased dead volumes from pipes, valves and tanks. Generally, the commercial production set up is very different to a laboratory set up. The optimized process parameters are very closely aligned with industrial production settings, that have been developed over years by trial-and-error. So, finding those optimal conditions (low salt elution conductivity in the 1st elution step to remove majority of impurities, effect of pH in the 1st elution step for effective removal impurities, effect of high salt elution for recovering LF with minimal impurities) took almost ten years. In contrast, predictive model-based optimization using GoSilico^{TM} Chromatography Modeling Software has taken less than 3 months with 9-12 laboratory experiments in small scale (27 mL column volume). Additionally, the predictive model showed further optimization potential for high salt elution conditions for minimising the salt usage, reducing the elution volume and increasing overall productivity.

The approach of combining traditional scale down experiments, keeping bed height and linear velocity constant, with mechanistic model-based process optimization shows a possible pathway for low cost, geographical independent, and rapid process development. The required lab-scale calibration experiments only took one day of experimental work and the subsequently obtained model based results showed a broad agreement with large scale experiments. Depending on the requirements this approach might be sufficient for the less regulated food industry.

If required predictive models can be used to further optimize process conditions at individual production sites to predict real time conditions. Like covering seasonal variation of milk composition, finding optimal loading capacity, and optimal elution volume to always work at the optimal commercial output, which can significantly increase revenue. For example, at an average lactoferrin production site, producing approximately 30 metric tons of lactoferrin per year an increase of only 1% in productivity would translate to an increased revenue of 0.25M USD per year at the current lactoferrin market price of 750 USD per kg, easily off-setting costs associated with model development. Therefore, this case study shows a possible simple implementation and the benefit of mechanistic modeling in process development strategies in the food industry.

CRediT authorship contribution statement

Lukas Gerstweiler: Conceptualization, Data curation, Formal analysis, Investigation, Methodology, Project administration, Resources, Visualization, Supervision, Writing – original draft. **Paulina Schad:** Investigation, Writing – review & editing. **Tatjana Trunzer:** Conceptualization, Methodology, Writing – review & editing. **Lena Enghauser:** Conceptualization, Writing – review & editing. **Max Mayr:** Conceptualization, Methodology, Writing – review & editing. **Jagan Billakanti:** Conceptualization, Methodology, Writing – review & editing.

Declaration of Competing Interest

The authors declare the following financial interests/personal relationships which may be considered as potential competing interests:

Lukas Gerstweiler reports equipment, drugs, or supplies was provided by Cytiva. Tatjana Trunzer reports a relationship with Cytiva that includes: employment. Lena Enghauser reports a relationship with Cytiva that includes: employment. Max Mayr reports a relationship with Cytiva that includes: employment. Jagan Billakanti reports a relationship with Cytiva that includes: employment.

Data availability

Data will be made available on request.

Acknowledgements

This work was supported by Cytiva Life Sciences by providing the GoSilico^{TM} software license and lab consumables.

Supplementary materials

Supplementary material associated with this article can be found, in the online version, at doi:10.1016/j.icarus.2017.10.034.

References

[1] H.M. Baker, E.N. Baker, A structural perspective on lactoferrin function, Biochem. Cell. Biol. 90 (3) (2012) 320–328, https://doi.org/10.1139/o11-071.
[2] I. Franco, M.D. Perez, C. Conesa, M. Calvo, L. Sanchez, Effect of technological treatments on bovine lactoferrin: An overview, Food Res. Int. 106 (2018) 173–182, https://doi.org/10.1016/j.foodres.2017.12.016.
[3] P.L. Masson, J.F. Heremans, Lactoferrin in milk from different species, Comp. Biochem. Physiol. B. 39 (1) (1971) 119–129, https://doi.org/10.1016/0305-0491(71)90258-6.
[4] J. Billakanti, Extraction of High-Value Minor Proteins from Milk, (2009). https://doi.org/10.26021/3347.
[5] Z. Yang, R. Jiang, Q. Chen, J. Wang, Y. Duan, X. Pang, S. Jiang, Y. Bi, H. Zhang, B. Lonnerdal, J. Lai, S. Yin, Concentration of Lactoferrin in Human Milk and Its Variation during Lactation in Different Chinese Populations, Nutrients 10 (9) (2018), https://doi.org/10.3390/nu10091235.
[6] Fortune Business Insights, Bovine lactoferrin market size, share and COVID-19 impact analysis by product, by application and regional forecast, 2022-2029, (report ID: FB1101656), 2021.
[7] H. Wakabayashi, K. Yamauchi, F. Abe, Quality control of commercial bovine lactoferrin, Biometals 31 (3) (2018) 313–319, https://doi.org/10.1007/s10534-018-0098-2.
[8] J. Billakanti, J. McRae, M. Mayr, K. Johnson, Advanced analytical tools for bovine lactoferrin identification and quantification in raw skim milk to finished lactoferrin powders, Internat. Dairy J. 99 (2019), https://doi.org/10.1016/j.idairyj.2019.104546.
[9] E. Krolitzki, S.P. Schwaminger, M. Pagel, F. Ostertag, J. Hinrichs, S. Berensmeier, Current practices with commercial scale bovine lactoferrin production and alternative approaches, Internat. Dairy J. 126 (2022), https://doi.org/10.1016/j.idairyj.2021.105263.
[10] L.K. Shekhawat, A.S. Rathore, An overview of mechanistic modeling of liquid chromatography, Prep. Biochem. Biotech. 49 (6) (2019) 623–638, https://doi.org/10.1080/10826068.2019.1615504.
[11] V. Kumar, A.M. Lenhoff, Mechanistic Modeling of Preparative Column Chromatography for Biotherapeutics, Annu. Rev. Chem. Biomol. Eng. 11 (2020) 235–255, https://doi.org/10.1146/annurev-chembioeng-102419-125430.
[12] C.R. Bernau, M. Knodler, J. Emonts, R.C. Japel, J.F. Buyel, The use of predictive models to develop chromatography-based purification processes, Front Bioeng. Biotechnol. 10 (2022), 1009102, https://doi.org/10.3389/fbioe.2022.1009102.
[13] P. Baumann, J. Hubbuch, Downstream process development strategies for effective bioprocesses: Trends, progress, and combinatorial approaches, Eng. Life Sci. 17 (11) (2017) 1142–1158, https://doi.org/10.1002/elsc.201600033.
[14] D. Saleh, G. Wang, F. Rischawy, S. Kluters, J. Studts, J. Hubbuch, In silico process characterization for biopharmaceutical development following the quality by design concept, Biotechnol. Prog. 37 (6) (2021) e3196, https://doi.org/10.1002/btpr.3196.
[15] L.K. Shekhawat, A.S. Rathore, Mechanistic modeling based process analytical technology implementation for pooling in hydrophobic interaction chromatography, Biotechnol. Prog. 35 (2) (2019) e2758, https://doi.org/10.1002/btpr.2758.
[16] S. Leweke, E. von Lieres, Chromatography Analysis and Design Toolkit (CADET), Computers Chem. Eng. 113 (2018) 274–294, https://doi.org/10.1016/j.compchemeng.2018.02.025.
[17] G. Guiochon, A. Felinger, D.G.G. Shirazi, Fundamentals of Preparative and Nonlinear Chromatography, 2nd Edition, Elsevier, 2006.
[18] H.S.-T.M.S.A. Seidel-Morgenstern, Preparative Chromatography, Wiley-VCH Verlag GmbH & Co. KGaA, 2020, https://doi.org/10.1002/9783527816347.
[19] C.A. Brooks, S.M. Cramer, Steric mass-action ion exchange: Displacement profiles and induced salt gradients, AIChE J. 38 (12) (1992) 1969–1978, https://doi.org/10.1002/aic.690381212.

[20] T. Hahn, P. Baumann, T. Huuk, V. Heuveline, J. Hubbuch, UV absorption-based inverse modeling of protein chromatography, Eng. Life Sci. 16 (2) (2016) 99–106, https://doi.org/10.1002/elsc.201400247.
[21] S. Hunt, T. Larsen, R. Todd, Modeling Preparative Cation Exchange Chromatography of Monoclonal Antibodies, Preparative Chromatography for Separation of Proteins, John Wiley & Sons2017. https://doi.org/10.1002/9781119031116.ch13.
[22] Cytiva, GoSilico Chromatography Modeling Software Software Help 29707122 AG, 2023.
[23] T. Hahn, Advances in Model-based Downstream Process Development, (2015). https://doi.org/10.5445/IR/1000051444.
[24] Z.H. Qureshi, T.S. Ng, G.C. Goodwin, Optimum experimental design for identification of distributed parameter systems, Internat. J. Control 31 (1) (2007) 21–29, https://doi.org/10.1080/00207178008961025.
[25] F. Gritti, G. Guiochon, Mass transfer kinetics, band broadening and column efficiency, J. Chromatogr. A. 1221 (2012) 2–40, https://doi.org/10.1016/j.chroma.2011.04.058.
[26] F. Gritti, T. Farkas, J. Heng, G. Guiochon, On the relationship between band broadening and the particle-size distribution of the packing material in liquid chromatography: theory and practice, J. Chromatogr. A. 1218 (45) (2011) 8209–8221, https://doi.org/10.1016/j.chroma.2011.09.034.
[27] S. Felletti, M. Catani, G. Mazzoccanti, C. De Luca, G. Lievore, A. Buratti, L. Pasti, F. Gasparrini, A. Cavazzini, Mass transfer kinetics on modern Whelk-O1 chiral stationary phases made on fully- and superficially-porous particles, J. Chromatogr. A. 1637 (2021), 461854, https://doi.org/10.1016/j.chroma.2020.461854.
[28] C.B. Colby, B.K. O'Neill, F. Vaughan, A.P.J. Middelberg, Simulation of Compression Effects during Scaleup of a Commercial Ion-Exchange Process, Biotechnol. Prog. 12 (5) (1996) 662–681, https://doi.org/10.1021/bp960051t.
[29] C.B. Colby, B.K. O'Neill, A.P.J. Middelberg, A Modified Version of the Volume-Averaged Continuum Theory To Predict Pressure Drop across Compressible Packed Beds of Sepharose Big-Beads SP, Biotechnol. Prog. 12 (1) (1996) 92–99, https://doi.org/10.1021/bp950029k.
[30] B. Guélat, L. Delegrange, P. Valax, M. Morbidelli, Model-based prediction of monoclonal antibody retention in ion-exchange chromatography, J. Chromatography A. 1298 (2013) 17–25, https://doi.org/10.1016/j.chroma.2013.04.048.
[31] M. Schmidt, M. Hafner, C. Frech, Modeling of salt and pH gradient elution in ion-exchange chromatography, J. Sep. Sci. 37 (1-2) (2014) 5–13, https://doi.org/10.1002/jssc.201301007.
[32] F. Rischawy, D. Saleh, T. Hahn, S. Oelmeier, J. Spitz, S. Kluters, Good modeling practice for industrial chromatography: Mechanistic modeling of ion exchange chromatography of a bispecific antibody, Comput. Chem. Eng. 130 (2019), https://doi.org/10.1016/j.compchemeng.2019.106532.
[33] Y. Yamamoto, T. Yajima, Y. Kawajiri, Uncertainty quantification for chromatography model parameters by Bayesian inference using sequential Monte Carlo method, Chem. Eng. Res. Des. 175 (2021) 223–237, https://doi.org/10.1016/j.cherd.2021.09.003.
[34] D. Saleh, G. Wang, B. Muller, F. Rischawy, S. Kluters, J. Studts, J. Hubbuch, Straightforward method for calibration of mechanistic cation exchange chromatography models for industrial applications, Biotechnol. Prog. 36 (4) (2020) e2984, https://doi.org/10.1002/btpr.2984.
[35] A. Osberghaus, S. Hepbildikler, S. Nath, M. Haindl, E. von Lieres, J. Hubbuch, Determination of parameters for the steric mass action model–a comparison between two approaches, J. Chromatogr. A. 1233 (2012) 54–65, https://doi.org/10.1016/j.chroma.2012.02.004.
[36] V. Kumar, S. Leweke, W. Heymann, E. von Lieres, F. Schlegel, K. Westerberg, A. M. Lenhoff, Robust mechanistic modeling of protein ion-exchange chromatography, J. Chromatogr. A. 1660 (2021), 462669, https://doi.org/10.1016/j.chroma.2021.462669.
[37] T. Briskot, T. Hahn, T. Huuk, J. Hubbuch, Protein adsorption on ion exchange adsorbers: A comparison of a stoichiometric and non-stoichiometric modeling approach, J. Chromatogr. A. 1653 (2021), 462397, https://doi.org/10.1016/j.chroma.2021.462397.
[38] O. Khanal, V. Kumar, F. Schlegel, A.M. Lenhoff, Estimating and leveraging protein diffusion on ion-exchange resin surfaces, Proc. Natl. Acad. Sci. USA 117 (13) (2020) 7004–7010, https://doi.org/10.1073/pnas.1921499117.
[39] K. Broeckhoven, D. Cabooter, F. Lynen, P. Sandra, G. Desmet, Errors involved in the existing B-term expressions for the longitudinal diffusion in fully porous chromatographic media Part II: experimental data in packed columns and surface diffusion measurements, J. Chromatogr. A. 1188 (2) (2008) 189–198, https://doi.org/10.1016/j.chroma.2008.02.058.
[40] S. Felletti, C. De Luca, G. Lievore, T. Chenet, B. Chankvetadze, T. Farkas, A. Cavazzini, M. Catani, Shedding light on mechanisms leading to convex-upward van Deemter curves on a cellulose tris(4-chloro-3-methylphenylcarbamate)-based chiral stationary phase, J. Chromatogr. A. 1630 (2020), 461532, https://doi.org/10.1016/j.chroma.2020.461532.
[41] J.B. Cheng, J.Q. Wang, D.P. Bu, G.L. Liu, C.G. Zhang, H.Y. Wei, L.Y. Zhou, J. Z. Wang, Factors affecting the lactoferrin concentration in bovine milk, J. Dairy. Sci. 91 (3) (2008) 970–976, https://doi.org/10.3168/jds.2007-0689.